The Journal of Eukaryotic Microbiology

ISOP Published by the International Society of Protistologists

Journal of Eukaryotic Microbiology ISSN 1066-5234

ORIGINAL ARTICLE

Molecular and Morphological Characterization of *Anncaliia azovica* sp. n. (Microsporidia) Infecting *Niphargogammarus intermedius* (Crustacea, Amphipoda) from the Azov Sea

Yuri S. Tokarev[a], Yuliya Y. Sokolova[b,c], Aleksandra A. Vasilieva[a,d] & Irma V. Issi[a]

a All-Russia Institute for Plant Protection, Russian Academy of Sciences, 3 Shosse Podbelskogo, Pushkin-St. Petersburg, 189620, Russia
b Institute of Cytology, Russian Academy of Sciences, 4 Tikhoretsky Avenue, St. Petersburg, 194064, Russia
c Microscopy Center, Department of Comparative Biological Sciences, School of Veterinary Medicine, Louisiana State University, 1909 Skip Bertman Drive, Baton Rouge, Louisiana 70803
d Peter the Great St. Petersburg Polytechnic University, 29 Politechnicheskaya ul., St. Petersburg, 195251, Russia

Keywords
Molecular phylogeny; multilocus sequence typing; natural host range; parasite prevalence; ultrastructure.

Correspondence
Y.Y. Sokolova, Microscopy Center, Department of Comparative Biomedical Sciences, School of Veterinary Medicine, Louisiana State University, 1909 Skip Bertman Drive, Baton Rouge, LA 70803, USA
Telephone/Fax number: +1-225-578-9899;
e-mail: sokolova@lsu.edu

Received: 26 June 2017; revised 6 September 2017; accepted September 8, 2017.
Early View publication October 9, 2017

doi:10.1111/jeu.12473

ABSTRACT

Five out of one hundred adults of *Niphargogammarus intermedius* caught at the Azov sea shore were found to be infected with microsporidia. The infection was found in the subcuticular fat body and myocytes. Parasites developed in direct contact with host cells, displayed a disporoblastic sporogony and diplokaryotic arrangement of nuclei at all stages. Spores were oval, 4.6–5.8 × 2.6–3.0 μm. Exospore appendages, vesicular–tubular secretions, and the anisofilar polar filament indicated a similarity to *Anncaliia* species. Sporont surfaces displayed ridges of amorphous material. Meronts and sporonts formed protoplastic extensions, similar to *A. vesicularum* and *A. meligheti*. Mature spores possessed a bipartite polaroplast. The polar tube was arranged in one row of 13–18 coils including 0–3 distal coils of lesser diameter. Partial sequencing of SSU, ITS, and LSU regions of rRNA gene (GenBank accessions: KY288064–KY288065) confirmed this new species to be congeneric with *A. algerae* (#AF069063) and *A. meligheti* (#AY894423). The SSU gene of this novel microsporidium shared 99.4% sequence similarity to *A. algerae* and 98.9% to *A. meligheti*. Genes for HSP70 and RPB1 amplified with primers designed for *A. algerae* orthologs displayed 99.7% and 97.4% similarity, respectively, between *A. algerae* and the novel microsporidium. A new species, *Anncaliia azovica*, is described based on morphological and molecular characterization.

MICROSPORIDIA are ubiquitous parasites of bilateral animals most frequently described from arthropods and fish. In many species of terrestrial and aquatic arthropods, microsporidia significantly impact host survival and fitness, and may cause severe epizootics leading to host population declines or devastation of cultivated hosts' colonies, with significant damage to beekeeping, sericulture, and aquaculture (Becnel and Andreadis 1999, 2014; Fries 2010; Stentiford et al. 2013). Microsporidia are also important pathogens of wild and farmed fish (Kent et al. 2014). Only less than 1% (14) of the known species (> 1,400) have been found in warm-blooded vertebrates, birds, and mammals. This strongly suggests that microsporidia have evolved primarily as parasites of invertebrates and fish, and that elevated body temperatures and adaptive immunity served the barriers that banned the majority of microsporidia, with the exception of *Enterocytozoon bieneusi* and *Encephalitozoon* spp., to become natural parasites of warm-blooded animals. However, among insect–parasitic microsporidia there are three groups, namely, the *Cystosporogenes/Endoreticulatus/Vittaforma*, the *Trachipleistophora/Vavraia*, and the *Anncaliia/Tubulinosema* clades that contain species with broad range of hosts, some of which tolerate high temperatures. These species under certain circumstances, particularly in the case of the host immunodeficiency or facilitated access to the immune privileged sites (like eyes), may infect birds and mammals. Potential sources of human infections with microsporidia from invertebrate hosts are likely associated with the species belonging to these three lineages (Sokolova 2015). In fact, each of them does include species that have been recorded to infect immunodeficient and rarely

immunocompetent humans or other mammals (Pariyakanok et al. 2015; Suankratay et al. 2012; Vávra et al. 1998, 2006, 2011; Weidner et al. 1999; Weiss 2014). Speaking specifically of the *Anncaliia/Tubulinosema* clade, *Tubulinosema acridophagus* from an American locust *Schistocerca americana* was found to cause myositis and disseminated infection in a patient with a bone marrow transplant (Choudhary et al. 2011; Meissner et al. 2012; Weiss 2014). *Anncaliia* (=*Brachiola*) algerae, a common parasite of several genera of mosquitoes (Andreadis 2007), occasionally infects brain and eye tissues and causes disseminated disease in immunocompromised individuals. *Anncaliia algerae* also may induce skin and muscle infections, presumably transmitted by a mosquito vector in immunologically healthy humans (Weiss 2014). In addition, *A. algerae* is known to develop infections in SCID mice (Koudela et al. 2001) and can be grown in insect (Visvesvara et al. 1999), fish (Monaghan et al. 2011), and mammalian (Trammer et al. 1999) cell cultures. The temperatures > 36 °C, which are required for mammalian cell growth, can be easily tolerated by *A. algerae*. Two representatives of the genus, *A. connori* and *A. vesicularum*, have been recorded only from humans with immunodeficiency, and their environmental source is unknown (Weiss 2014). Other *Anncaliia* spp. parasitize insects. *Anncaliia gambiae*, like *A. algerae*, infects dipterans (Weizer, Žižka 2004), and *A. varivestis* and *A. meligheti*—coleopterans (Brooks et al. 1985; Issi et al. 1993. Here we describe a new species *Anncaliia azovica* from an amphipod *Niphargogammarus intermedius*. This first finding of a microsporidium belonging to the *Anncaliia/Tubulinosema* clade in crustaceans further widens the host range of the "generalist" genus *Anncaliia*.

MATERIALS AND METHODS

Sampling and light microscopy

In June 2013, numerous gammarids were observed at the intertidal zone of Azov sea shore in the vicinity of village Achuevo, Slavyansk District of Krasnodar Territory in the South-Western part of Russia. Adult gammarids were recovered at the territory of a public beach (45°42′30″ N, 37°44′00′ E0) and examined visually using illumination with transmitted light. The arthropods showing unusual swelling of inner tissues were dissected and examined by bright-field light microscopy, which revealed presence of multiple oval spores. The smears were methanol fixed and stained with 5 mM DAPI for fluorescent microscopy. The inner tissues from the infected specimens were further processed either for electron microscopy or for DNA extraction as described elsewhere (Tokarev et al. 2010). The remaining 95 specimens did not show inner tissue swelling and no spores were identified upon microscopic examination. Ethanol-fixed gammarids were submitted for identification to the Institute of Zoology, Russian Academy of Sciences, St. Petersburg, and were identified as *N. intermedius* Carausu 1943 using a field guide by Mordukhai-Boltovskoi et al. (1969) as a key.

Electron microscopy

For transmission electron microscopy (TEM), in 2 wk after fixation, the samples were cut in smaller pieces, transferred to fresh portion of fixative for 2 h, washed in 0.1 M cacodylate buffer supplemented with 5% sucrose, post-fixed in 2% osmium tetroxide, dehydrated in ascending ethanol series, transferred to propylene oxide, and embedded in Epon-Araldite. Thin (70–80 nm) sections were stained with uranyl acetate and Reynolds' lead citrate and examined in JEOL JEM 1011 transmission electron microscope equipped with HAMAMATSU ORCA-HR digital camera (Tokyo, Japan). For scanning electron microscopy (SEM), specimens were fixed with glutaraldehyde only, dehydrated through the ethanol series, followed by exchanging ethanol with CO_2 in Polaron E3000 Standard Critical Point Drier. Dried samples were mounted on 13 mm aluminum mount specimen stubs covered with carbon adhesive tabs, sealed with colloidal silver paste, coated with Gold/Palladium in EMS 550X Sputter Coater for 4 min to achieve the thickness of coating 20–25 nm, and examined in Fei Quanta 200 ESEM in a high vacuum mode at 20 kV. All reagents for LM were from Sigma-Aldrich (St. Louis, MO), and for EM from EMS Chemicals (Fort Washington, PA).

PCR amplification and phylogenetic analyses

PCR was run using a Bio-Rad MyCycler DNA amplifier in 20 μl volume containing 10 μl DNA template, PCR buffer, 0.25 mM dNTPs, 1 U Taq-polymerase (Sileks, Russia), and 0.5 pMol each of forward and reverse primers (Evrogen, Russia). For species identification of microsporidia, a set of universal microsporidia primer combinations (18f:1047r; 530f:1492r; 1129f:ls580r), spanning three respective overlapping regions of small subunit (SSU), internal transcribed spacer (ITS), and large subunit (LSU) ribosomal RNA (rRNA) gene, was exploited (Weiss and Vossbrinck 1999). Primers amplifying 500- to 700-bp-long fragments of genes coding heat shock protein (HSP70) and largest subunit RNA polymerase II (RPB1) were designed basing on *A. algerae* orthologs (Table 1). PCR reactions included initial denaturation (95 °C for 3 min), 30 amplification cycles (denaturation at 95 °C for 30 s, annealing at 54 °C for 30 s, elongation at 72 °C for 60 s), and a final extension step (72 °C for 5 min). PCR products were separated by agarose gel electrophoresis. The gel regions containing specific products were excised, melted with 3 M GITC buffer at 60 °C, and mixed with an aliquot of silica particles subsequently precipitated by centrifugation and washed with a washing buffer (10 mM Tris, pH 7.5, 50 mM NaCl, 25 mM EDTA, and 50% ethanol) and 96° ethanol. DNA fragments were eluted by molecular-grade deionized water, checked for quantity by electrophoresis using a MassRuler Low Range DNA Ladder (Thermo Scientific, Waltham, MA) as a standard, and sequenced with Abi Prism Genetic Analyzer 3500 in both directions. The obtained sequences were aligned, corrected in BioEdit v7.0.8.0 (Hall 1999), and compared to the orthologs

Table 1. Primers designed in the present study for genotyping the new microsporidium and its host *Niphargogammarus intermedius*

Primer name	5′–3′ Sequence	GC, %	Tm, °C	Product size, bp	Amplified locus
AncHSP70for1	CTCTGCTCCAAATATTTCGATAGAGC	42	62	610	Heat shock protein (HSP70) of *Anncaliia*
AncHSP70rev1	AAACATCCTGAATGATCAACCTCAC	40	62		
AncRPB1for1	TGATTGCACTACCTCTGTTATTCCTG	42	63	735	Large subunit of RNA polymerase
AncRPB1rev1	TGAATTGATAATAACGCCTTGAATTTCTCT	30	62		II (RPB1) of *Anncaliia*

available in GenBank using built-in BLAST utility. For the SSU rRNA gene-based phylogeny, the newly obtained sequence and GenBank-accessible sequences of related microsporidia (Table 2) were aligned in BioEdit. Regions containing gaps and ambiguous sites were removed. In the final data set, the length of the aligned regions was 909 bp. Phylogenetic reconstructions were performed using the maximum likelihood (ML) method based on Tamura-Nei model in MEGA 7 (Kumar et al. 2015) and Bayesian inference (BI) basing on GTR + I + G model in MrBayes v3.1.2 (Ronquist et al. 2012). Pairwise evolutionary distances were estimated by Kimura-2 parameter algorithm (Kimura 1980; Tamura et al. 2011).

RESULTS

Gross pathology and light microscopy

Five out of 100 examined *N. intermedius* adults, showed swelling of inner tissues, visible by unaided eye in transmitted light (Fig. 1). The swollen tissues were opaque. Light microscopy of dissected tissues in all five specimens demonstrated the presence of numerous oval spores of uniform shape and size, typical for microsporidian infections. Unfixed spores measured 4.6–5.8 (5.1 ± 0.06) × 2.6–3.0 (2.8 ± 0.03) μm ($N = 20$), methanol fixed—4.5–5.7 (4.9 ± 0.08) × 2.4–3.2 (2.8 ± 0.04) μm ($N = 20$) with average spore index (length/width ratio) of 1.8. DAPI staining of methanol-fixed spores showed diplokaryotic arrangement of nuclei (Fig. 1).

Ultrastructure of the life cycle stages

Sections through the infected gammarid revealed that the layer underlying subcuticular epithelium normally occupied by subcuticular fat body was completely replaced by mature microsporidian spores, rare presporogonial developmental stages, and electron-dense deposits of the parasite secretion. The space surrounding parasites was electron transparent and devoid of any remnants of host cells (Fig. 2a). Within the musculature, the infected regions were patchily distributed corresponding probably to the individual heavily infected myocytes. The latter were filled predominantly with proliferating sporonts and star-shaped sporoblasts, but not with mature spores. This suggests that the infection might have started from the subcuticular fat body, and the myocytes were the secondary infection site. Spores were rarely seen on sections through infected muscles (Fig. 2b). Examination of infected tissues with the scanning electron microscope (SEM) revealed spores residing among muscle fibers (Fig. 2c).

The earliest observed stage was a diplokaryotic meront (Fig. 2d) of irregular shape with cytoplasmic protrusions penetrating into the host cytoplasm (Fig. 2d, e). The similar structures termed "protoplasmic extentions" (Cali et al. 1998) were observed in *A. vesicularum* (Cali et al. 1998) and *A. meligheti* (Franzen et al. 2006). The circular profiles submerged into electron-dense matrix of the meront envelop (Fig. 2d–g) were occasionally seen on sections and matched the descriptions of "vesicular–tubular

Table 2. Microsporidia species, names, and taxonomic position of hosts and GenBank entries used for small subunit rRNA gene-based phylogenetic reconstructions

Microsporidia species	Host	GenBank accession number
Anncaliia azovica sp. n.	*Niphargogammarus intermedius* (Amphipoda: Gammaridae)	KY288064
Anncaliia (*Nosema*) *algerae*	*Anopheles stephensi* (Diptera: Culicidae)	AF069063
Anncaliia meligheti	*Melighetes aeneus* (Coleoptera: Nitidulidae)	AY894423
Janacekia debaisieuxi	*Simulium* sp. (Diptera: Simulidae)	AJ252950
Kneallhazia carolinensae	*Solenopsis carolinensis* (Hymenoptera: Formicidae)	GU173849
Kneallhazia solenopsae	*Solenopsis invictae* (Hymenoptera: Formicidae)	AY312502
Tubulinosema acridophagus	*Schistocerca americana* (Orthoptera: Acrididae)	AF024658
Tubulinosema hippodamiae	*Hippodamia convergens* (Coleoptera: Coccinellidae)	JQ082890
Tubulinosema kingi	*Drosophila willistoni* (Diptera: Drosophilidae)	DQ019419
Tubulinosema loxostegi	*Loxostege sticticalis* (Lepidoptera, Crambidae)	JQ906779
Tubulinosema pampeana	*Bombus atratus* (Hymenoptera: Apidae)	KM883008
Tubulinosema ratisbonensis	*Drosophila melanogaster* (Diptera: Drosophilidae)	AY695845
Visvesvaria algerae	*Anopheles stephensi* (Diptera: Culicidae)	AF024656

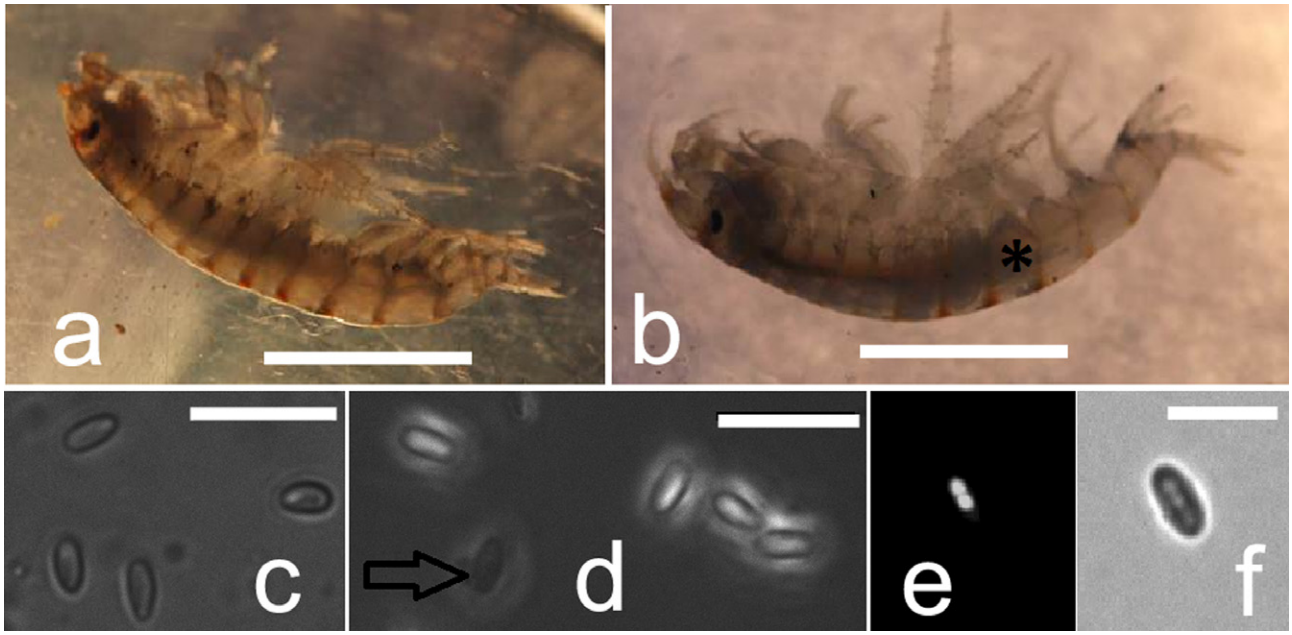

Figure 1 Gross pathology and light microscopy of *Anncaliia azovica* infection. (**a**) Uninfected *Niphargogammarus intermedius*. (**b**) Infected *N. intermedius* with slightly swollen inner tissues (asterisk). (**c** and **d**) Unfixed spores and (**e, f**) methanol-fixed DAPI-stained spores. (c, f) Bright field, (d) phase contrast, (e) epifluorescence microscopy. The arrow indicates an empty spore. Scale bars: a and b, 2 mm; c and d, 10 μm; e and f, 5 μm.

appendages" or "vesicular–tubular secretion" (Cali et al. 1998, 2004) observed at proliferative stages in all representatives of the genus *Anncaliia* studied ultrastructurally (Brooks et al. 1985; Cali et al. 1998, 2004; Canning and Sinden 1973; Franzen et al. 2006; Issi et al. 1993). Sections through meronts demonstrated electron-lucid cytoplasm with numerous cisternae of endoplasmic reticulum, and diplokarya, often in the process of mitosis. Vesicular–tubular appendages were seen on sections as circular profiles. They were often grouped in chains, some of which were attached to the parasite envelope (Fig. 2e–h).

Sporonts, the proliferative stage that follows the meront in the life cycle, exhibited more electron-dense cytoplasm, slightly thicker envelope, and occasional circular structures attached to the surface (Fig. 2i–l, 3a). A few sporonts demonstrated protoplastic extentions, in some of which peculiar net-like fenestrated membrane structures were seen (Fig. 2i). The amorphous electron-dense material deposited on the sporont surface and formed "ridges" (Cali et al. 1998), which were well seen only at the particular plane of tangential sections (Fig. 2j, k), and on transverse sections appeared as broad indentation of the electron-dense envelope (Fig. 3a). Vesicular–tubular elements were submerged in this surface material but were hardly seen being obliterated by amorphous secretion (Fig. 2k). Chains of circular structures were often seen detached from the sporont surfaces, and clustered in electron-dense globules up to 500 nm in diameter (Fig. 2k, 3a). A massive tubular Golgi organelle was seen in some sporonts in vicinity of a diplokaryon (Fig. 2l). We never observed sporonts with more than 2 diplokarya, suggestive of synchronization of the nuclear and cell divisions. The most typical were elongated cells with one centrally or eccentrically located diplokaryon (Fig. 3a).

Sporoblasts were the cells with thick electron-dense envelopes corresponding to future exospores, underlain by a thin translucent layer, the endospore precursor. Sporoblasts did not divide and contained primordial polar tube coils arranged in one row (Fig. 3b). Characteristic features of the sporoblasts were "waving" cell contours ("star-shaped" cells) and sporadic vesicular–tubular appendages attached to the exospore (Fig. 3b, c). These appendages were also noticeable on the surface of some mature spores (Fig. 3d–h), though the surface of the fired spores was always smooth (Fig. 3i). Spores on thin sections measured 2.9–4.3 × 1.4–1.7 μm. The spore wall was composed of about 100-nm-thick (70–170 nm) endospore and about 50-nm-thick (44–46 nm) amorphous exospore occasionally encrusted with the elements of vesicular–tubular secretion appeared on sections as circular profiles 40–80 nm in diameter (Fig. 2g). On the apical pole the endospore was practically lacking, and the polar cap was closely adjacent to the exospore (Fig. 2d, e). Spores were diplokaryotic and contained a canonical set of microsporidian organelles (Fig. 2d–g). Polaroplast was composed of two regions: the anterior part built of tightly packed lamellae and the posterior one composed of saccules limited by the membrane. The latter was attached to the membrane enveloping the uncoiled region of the polar tube (Fig. 3f). Polar filament was composed of 13–17 coils (median = 15). It was slightly anisofilar with 0–4 (median = 3)

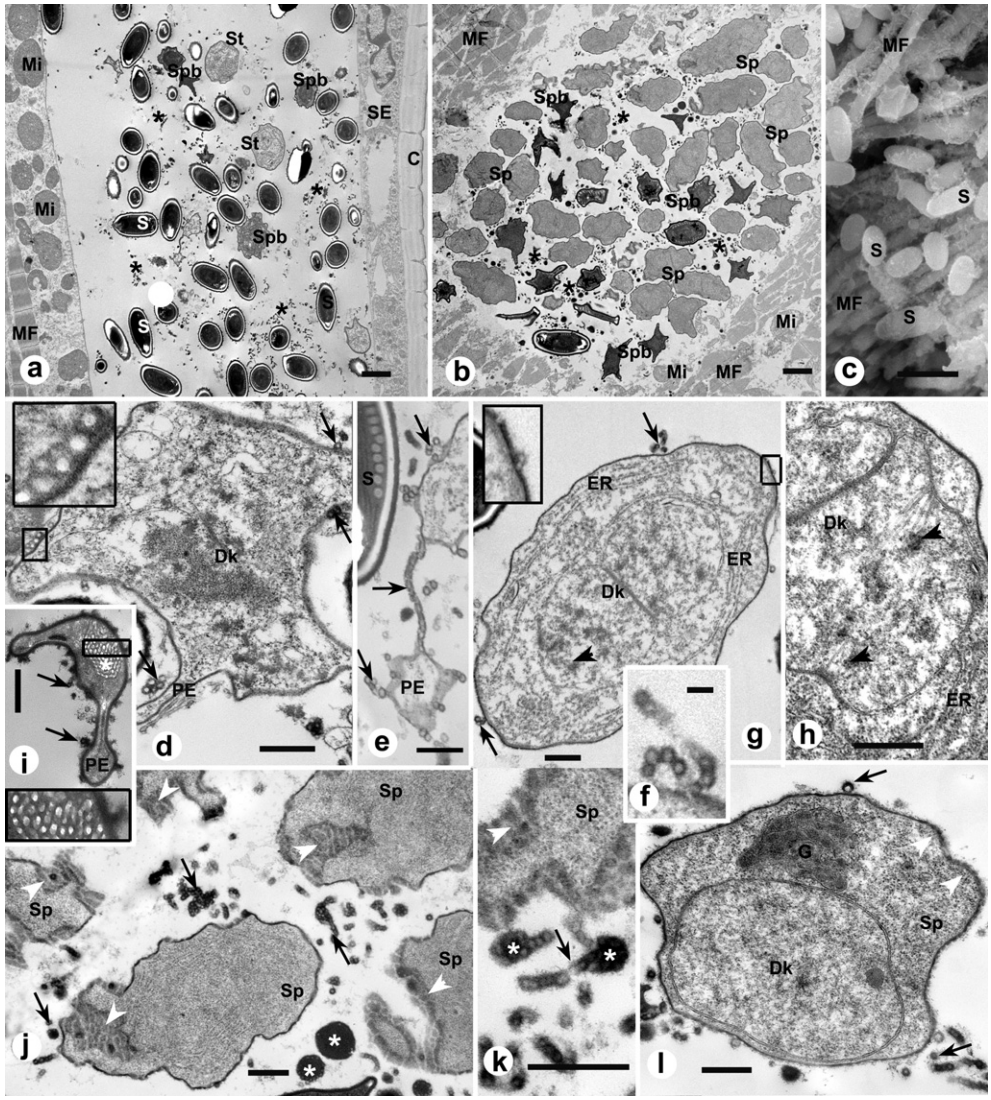

Figure 2 Electron microscopy of *Anncaliia azovica*: tissue tropism, ultrastructure of presporogonial stages, and secretion types. (**a**) The fat body layer underlying subcuticular epithelium normally occupied by adipocytes is replaced by numerous mature spores, rare prespore developmental stages, and deposits of the parasite secretion (asterisk). The layer devoid any remnants of host cells. (**b**) A section through thoracal musculature demonstrates an electron-lucid patch correspondent to an infected myocyte in which muscle fibers and other organelles have been substituted by developing microsporidia and their secretion (asterisk). Numerous sporonts, a few sporoblasts, and one mature spore are in the view. (**c**) Infected muscles in SEM: mature spores reside among muscle fibers. (**d**) The earliest observed stage, a diplokaryotic meront of irregular shape. Transversally sectioned tubules or vesicles seen as circular bodies (arrows), are submerged into electron-dense matrix of the meront envelope (boxed insert). "Protoplastic extensions," elongated portions of the parasite cytoplasm, penetrate deeply into the host cytoplasm. (**e**) Protoplasmic extension separated from the "mother cell" by narrow cytoplasmic bridge incrusted with vesicular–tubular secretion. (**f**) Chains of circular profiles, attached to the meront envelope ("vesicular–tubular secretion"). (**g** and **h**) Sections through diplokaryotic meronts demonstrating electron-lucid cytoplasm with numerous cisternae of endoplasmic reticulum, diplokaryon in the process of mitosis, and vesicular–tubular secretion on the surface (arrows). Condensed chromosomes attached to spindle microtubules, are indicated by arrowheads. (**i**) A sporont with a protoplastic extension and "MIN-like" fenestrated membrane structure (white asterisk, insert). (**j** and **k**) "Ridges" of electron-dense matrix on the surface of sporonts are visible at the particular plane of tangential sections through the sporont (white arrow). Vesicular–tubular secretion seen on sections as chains of circular profiles (black arrows), form electron-dense globules up to 500 nm in diameter (white asterisks). (**l**) An early sporont displaying denser cytoplasm comparatively to meronts and a massive Golgi organelle. Ridges on the surface are indicated by white arrowheads, circular profiles – by a black arrows. C = cuticle; DK = diplokaryon; ER = endoplasmic reticulum; MF = muscle fibers; Mi = mitochondria; S = spores; SE = subcuticular epithelium; Spb = sporoblast; St = meronts (early developmental stage). Scale bars: a and b, 2 μm; c, 5 μm; f, 100 nm; d and e, g–i, 500 nm.

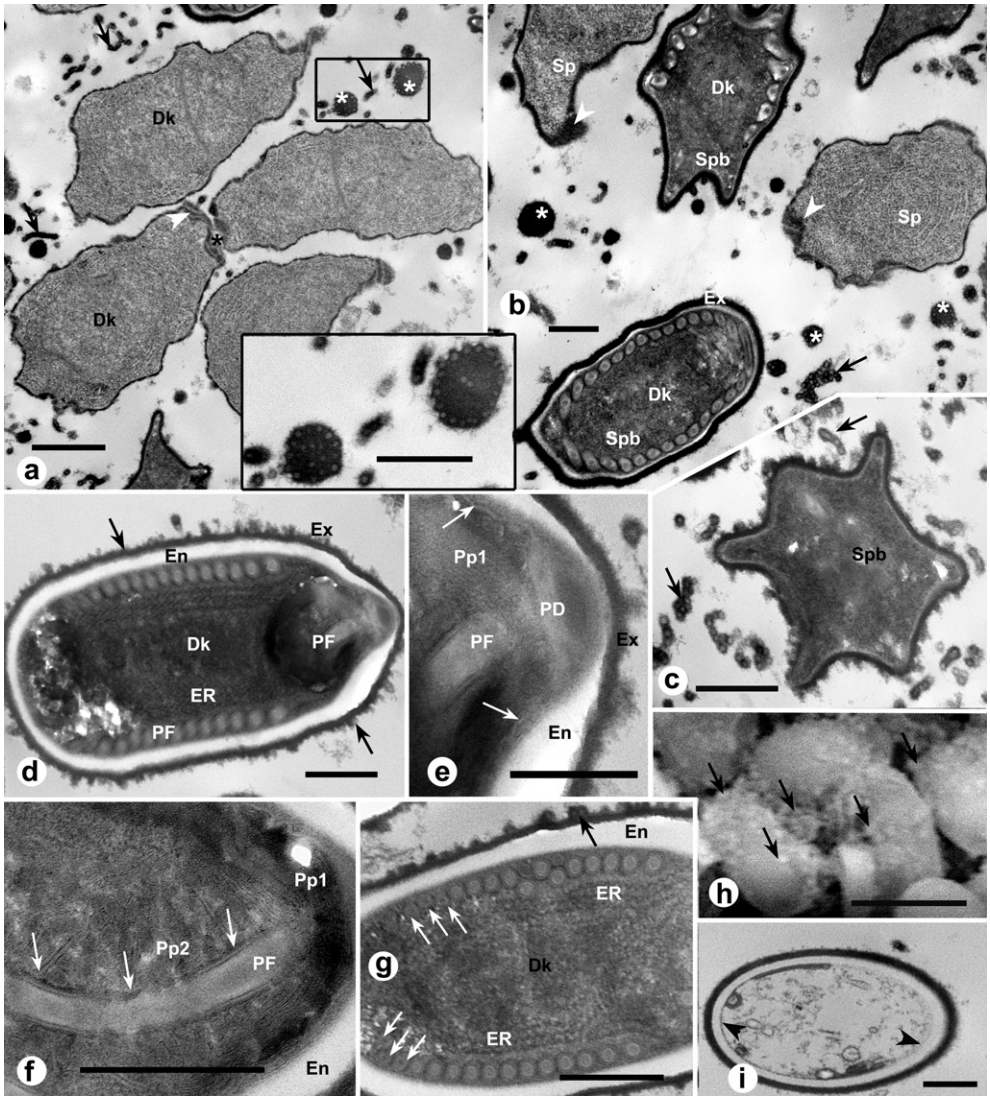

Figure 3 Electron microscopy of *Anncaliia azovica*: sporogony and spore ultrastructure. (**a**) Two recently divided diplokaryotic sporonts are still bound by the electron-dense material of their envelopes (black asterisk). Arrows indicate tubular–vesicular secretion abundant within the electron-lucid space surrounding sporonts. Boxed insert demonstrates electron-dense globules composed of whirled chains of tubular–vesicular profiles and amorphous electron-dense matrix (white asterisks). (**b**) Sporoblasts demonstrating a thick exospore, thin endospore, and polar tube precursor arranged in one row. Conglomerates of secreted material are indicated by white asterisks. (**c**) Cross-section through a typical "star-shaped" sporoblast with vesicular–tubular secretion (arrows) either attached to the sporoblast surface or freely residing in the surrounding host cell cytoplasm. (**d**) A longitudinal section through a diplokaryotic spore with canonical organelles. Black arrows point to the strands of amorphous material extending from the exospore surface. (**e**) Apical region of a spore showing a polar disc, polar sac (white arrows) and apical region of the polaroplast composed of tightly packed membranous lamellas. Note the absence of the endospore at the apical spore pole. (**f**) Section through a spore demonstrating structure of the polaroplast with the apical lamellae region (PP1) and the vacuolar part (PP2) composed of broad vacuoles attached to the membrane that encloses the uncoiled region of the polar filament (white arrows). (**g**) A section through a median part of the spore demonstrating diplokaryon and slightly anisofilar polar tube. White arrows indicate three posterior coils of smaller diameter. Black arrow indicates a circular profile attached to the exospore. (**h**) Scanning electron microscopy: arrows indicate blebs or vesicles on the surface of young spores corresponding to vesicular–tubular secretion seen on sections. (**i**) The empty spore shell (after the sporoplasm discharge) demonstrating a smooth exospore, plasmalemma (arrowheads) and internal membranes. En = endospore; ER = endoplasmic reticulum; Ex = exospore; PF = polar filament; Pp = polaroplast. Other abbreviations are the same as on the Fig. 2. Scale bars, a–g, i, 500 nm; h, 5 μm.

posterior coils of lesser diameter. Posterior vacuole was not visible. Examination of the surface of sporoblasts and spores in SEM clearly demonstrated that "vesicular–tubular" appendages seen on the surface of young spores and sporoblasts in TEM were in fact blebs or vesicles submerged in a fine matrix surrounding the surface. The vesicles were assembled in chains or globule structures. No tubules were seen in SEM (Fig. 3h).

PCR amplification, sequencing, and phylogenetic analysis

Although a positive PCR signal was achieved with all three primer sets, sequencing was successful only with 18f:1047r and 1129f:ls580r primer pairs. Primers 530f:1492r generated heterogeneous amplicons most likely due to nonspecific annealing of host genomic DNA. The resulting SSU (GenBank accession # KY288064), ITS, and LSU rRNA (# KY288065) were identical in both specimens (isolates AZG3 and AZG5) of the new microsporidium. These sequences showed high similarity to the reference records of *A. algerae* (# AF069063), *A. meligheti* (# AF024656), and *Visvesvaria algerae* (# AY894423). In detail, partial SSU rRNA gene sequence, 966 bp long, was 98.9% and 99.1% similar to the reference records of *A. algerae* and *A. meligheti*, respectively, which, in turn, were 98.8% similar to each other. Partial LSU rRNA gene sequence, 444 bp long, was 97.0% and 95.8% similar to respective *A. algerae* and *A. meligheti* sequences, which were 94.2% similar to each other. The 40-bp-long ITS sequence was the most variable, showing 85% and 70% similarity to the ITS region of *A. algerae* (Table 3) and *A. meligheti*, while the latter two were 97.2% similar to each other. Analysis of SSU rRNA gene sequence of *V. algerae* from *Anopheles stephensi* showed 98.8–98.9% similarity to the orthologs from *Anncaliia* spp. In phylograms obtained by Bayesian inference and maximum likelihood algorithms, these four species clustered together as expected for closely related members of one genus (Fig. 4). Pairwise evolutionary distances among four sequences of *Anncaliia* spp. ranged from 0.003 between the novel species and *A. meligheti* to 0.009 between *V. algerae* and *A. algerae*. Similar distance values (0.001–0.007) separated species of the genus *Tubulinosema*. The distances between *Anncaliia* spp. and *Tubulinosema* spp. (0.255–0.268) were greater that those separating *Anncaliia* spp. and *Kneallhazia* spp. (0.134–0.148) (Table 4).

For better understanding the genetic polymorphism within this group of microsporidia, partial sequences of genes encoding heat shock protein 70 (HSP70) and RNA polymerase (RPB1) were obtained and compared to the respective sequences of *A. algerae*. The HSP70 gene sequence of the described microsporidium, 555 bp long (GenBank accession number # KY288066), was 99.7% similar to that of *A. algerae*, while the translated protein sequence 185 amino acids long was identical in these two species, indicating high level of conservation of this locus, even higher than in SSU rRNA gene. The RPB1 gene sequence of the novel species (GenBank accession number # KY288067) was more variable, showing 97.4% and 96.7% similarity to *A. algerae* nucleotide (639 bp) and translated protein sequences (213 aa), respectively.

Table 3. Percentage of sequence similarity of the studied genes between *Anncaliia algerae* and *Anncaliia azovica* sp. n.

	Sequence similarity	
Locus	Nucleotide	Amino acid
SSU rRNA[a]	99.4	–
ITS	85.0	–
LSU rRNA	97.0	–
HSP70	99.7	100
RPB1	97.5	96.7

[a]SSU rRNA, small subunit ribosomal RNA gene; ITS, gene for internal transcribed spacer; LSU rRNA, large subunit ribosomal RNA gene; HSP70 and RPB1, abbreviated as in Table 1.

DISCUSSION

Phylogenetic analyses based on sequences of several genes unequivocally place the novel species on the branch of *Anncaliia* spp. This lineage belongs to the clade 3 and the superclade "Aquasporidia" that contains predominantly microsporidia-infecting hosts from freshwater habitat, with a few genera, like the closest to *Anncaliia*, *Tubulinosema*, and *Kneallhazia* that have switched to parasitism in terrestrial insects (Vossbrinck and Debrunner-Vossbrinck 2005). The position within the *Anncaliia* branch perfectly fits the morphological data. *Anncaliia* spp. described ultrastucturally, share several characters. These include thickened membrane at the proliferative stages, slightly anisofilar polar filament, and the presence of the secrete material derived from the surface of the parasite cells at the proliferative and sporogenic stages. This material in all *Anncaliia* spp. is composed of individual or aggregated vesicular–tubular structures seen on sections as electron-dense circular profiles with an electron-transparent core. In the newly described species, the circular profiles were present on the sections through envelopes of meronts, sporonts, sporoblasts, and young spores. Observation of the spore surface in scanning electron microscope suggests that the observed episporal structures are vesicles rather than tubules. However, it cannot be excluded that these structures are in fact varicose tubules composed of short thin-walled regions connecting thick-walled "knots," seen as vesicles (or circles on sections). Of seven so far described *Anncaliia* spp. (Table 5), three species including the one described herein, develop elongated cytoplasmic protrusions extended in the host cytoplasm at the proliferative stages, termed here and elsewhere "protoplasmic extensions" (Cali et al. 1998; Franzen et al. 2006). The fenestrated net-like structures that we observed on the periphery of some protoplastic extensions (Fig. 2i) resemble "vesicular–tubular caps" seen in *A. vesicularum* (Cali et al. 1998). These surface networks also display structural similarity with "MIN," the "Membrane Interlaced Network" (Cali et al. 2002; Takvorian et al. 2005), the organelle with Golgi functions (Takvorian et al. 2013) observed in sporoplasms of *A. algerae* (Cali et al. 2002; Takvorian et al. 2005) and *Kneallhazia solenopsae* (Sokolova and Fuxa 2008). These structures could represent a specialized secretory compartment that produces surface material at the certain phase of the microsporidium life cycle.

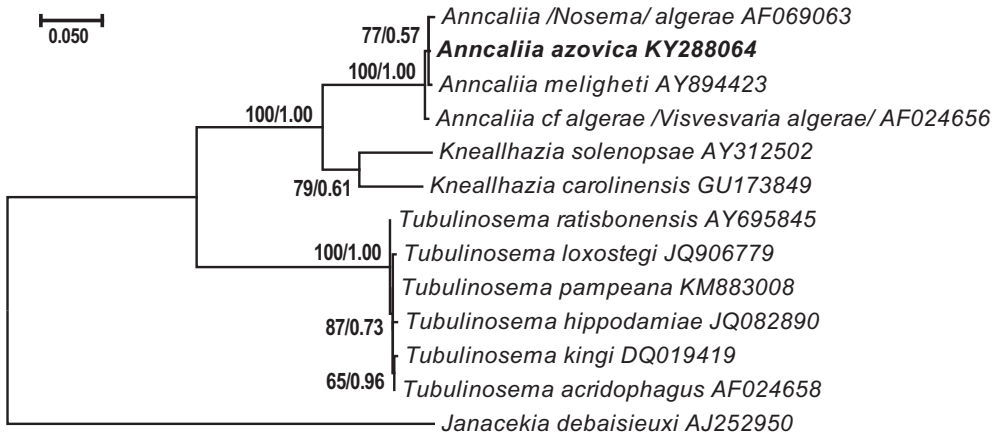

Figure 4 Small subunit ribosomal RNA gene-based phylogeny of *Anncaliia azovica* and allied species estimated by maximum likelihood (ML) and Bayesian inference (BI) methods. Each taxon is annotated with GenBank accession number. The scale bar is 0.05 expected nucleotide changes per site. Numbers at nodes correspond to the bootstrap support values for ML (left) and posterior probability values for BI (right).

Table 4. Estimates of pairwise evolutionary divergence among SSUrRNA gene sequences of *Anncaliia azovica* sp. n., its closest relatives, and *Janacekia debaisieuxi*, the outgroup, using Kimura 2-parameter model[a]

	Species name and GenBank accession number	1	2	3	4	5	6	7	8	9	10	11	12
1	*Anncaliia* (*Nosema*) *algerae* (AF069063)												
2	*Anncaliia* (*Visvesvaria*) *algerae* (AF024656)	0.009											
3	*Anncaliia meligheti* (AY894423)	0.007	0.008										
4	*Anncaliia azovica* sp. n. (KY288064)	0.006	0.007	0.003									
5	*Kneallhazia carolinensis* (GU173849)	0.138	0.135	0.134	0.135								
6	*Kneallhazia solenopsae* (AY312502)	0.148	0.143	0.144	0.146	0.096							
7	*Tubulinosema acridophagus* (AF024658)	0.265	0.260	0.261	0.258	0.240	0.238						
8	*Tubulinosema ratisbonensis* (AY695845)	0.261	0.257	0.258	0.255	0.239	0.234	0.003					
9	*Tubulinosema kingi* (DQ019419)	0.268	0.263	0.265	0.261	0.243	0.241	0.002	0.006				
10	*Tubulinosema hippodamiae* (JQ082890)	0.268	0.263	0.265	0.262	0.244	0.241	0.004	0.006	0.007			
11	*Tubulinosema loxostegi* (JQ906779)	0.266	0.261	0.263	0.260	0.242	0.240	0.003	0.004	0.006	0.006		
12	*Tubulinosema pampeana* (KM883008)	0.263	0.258	0.260	0.257	0.239	0.237	0.001	0.002	0.003	0.003	0.002	
13	*Janacekia debaisieuxi* (AJ252950)	0.399	0.393	0.397	0.399	0.409	0.392	0.397	0.391	0.401	0.401	0.395	0.395

[a]The numbers of base substitutions per site from between sequences are shown. There were a total of 899 positions in the final data set. Evolutionary analyses were conducted in MEGA7.

Based on ssrDNA analysis, this new species from *Niphargogammarus intermedius* differs from *A. algerae* by five nucleotides and from *Anncaliia meligheti* by eight nucleotides in the SSUrDNA region (968-bp-long alignment). SSUrDNA-based distance matrix analysis demonstrates that evolutionary distances between *Anncaliia* spp. are comparable to ones separating closely related species of other insect-infecting microsporidian genera, like *Nosema* (Kyei-Poku and Sokolova 2017), *Paranosema* (Sokolova et al. 2003), *Libermannia* (Sokolova et al. 2009), and *Tubulinosema* (herein, Table 4). Surprisingly, both phylogenetic and distance matrix analyses suggest that *Anncaliia* spp. is closer related to *Kneallhazia* spp. than to *Tubulinosema* sp. This corroborates with a unique morphological character, the presence of MIN-like structure in sporoplasms of *A. algerae* and *K. solenopsae* (Cali et al. 2002; Sokolova and Fuxa 2008). The presented phylogenetic analyses (Fig. 4 and Table 4) also implies that the sequence of *V. algerae* may belong to yet undescribed species of the genus *Anncaliia*, but not to *Anncaliia* (*Brachiola*) *algerae* as it was presumed by Franzen et al. (2006). The RPB1 gene of the novel species was successfully amplified and demonstrated greater divergence from the *A. algerae* ortholog than SSU genes. This indicates that the RPB1 gene may be used in future as an additional molecular marker for differentiation of closely related

Table 5. Diagnostic characters of *Anncaliia* spp.

Species name (original description)	Spore length × width, μm	Ultratructural characters: PFC (distal PFC), number	Ultratructural characters: 1. Protoplasmic extensions in M and Sp; 2. Ridges in Sp; 3. Exospore appendages in Spb and S; 4. Secretion type	Type host (Class, Order); other natural and experimental hosts	References
Anncaliia azovica sp. n	4.6–5.8 × 2.6–3.1	12–17 (0–4)	1.PE+ 2. R+; 3. VT in S and Spb; 4. V, VC, VG	*Niphargogammarus intermedius* (Crustacea, Amphipoda)	Here in
Anncaliia (=*Nosema, =Brachiola*) *algerae* (Vavra, Undeen, 1970)	3.7–5.4 × 2.3–3.9	8–11 (0–3)	1. PE-; 2. R+; 3. EA- 4. V, VC, VG	*Anopheles stephensi* (Insecta, Diptera); *Anopheles* spp., insects, amphipods, *Homo sapiens*[a], mice; mammal, fish and insect cells	Canning and Sinden (1973), Cali et al. (2004), Koudela et al. (2001), Trammer et al. (1999), Visvesvara et al. (1999) and Monaghan et al. (2011)
Anncaliia connori (=*Nosema, =Brachiola*) (Sprague, 1974)	4–5 × 2–2.5	10–12	No data	*Homo sapiens*[b] (Mammalia, Primates)	Margileth et al. (1973), Sprague (1974) and Shadduck et al. (1979)
Anncaliia (=*Brachiola*) *gambiae* (Weiser and Žižka, 2004)	2.5–3.0 × 1.5–2.0	9 (3–4)	1. PE-; 2. R-; 3. EA-; 4. V, VC, VG	*Anopheles gambiae* (Insecta, Diptera)	Weiser and Žižka (2004)
Anncaliia (=*Nosema*) *meligheti* (Issi, Radishcheva, 1979)	4–4.8 × 2–3	13–15 (3–4)	1. PE+; 2. R+ 3. T in S; 4. V, VC, VG	*Melighetes aeneus* (Insecta, Coleoptera); *Pieris brassicae*	Issi et al. (1993) and Franzen et al. (2006)
Anncaliia (=*Nosema*) *varivestis* (Brooks et al., 1985)	4.7 ± 0.06 × 2.6 ± 0.03	17–19	1. PE-; 2. R+; 3. EA- 4. T, V, VC, VG	*Epilachna varivestis* (Insecta, Coleoptera)	Brooks et al. (1985)
Anncaliia (=*Brachiola*) *vesicularum* (Cali et al., 1998)	2.5 × 2.0	7–10 (2–3)	1. PE+; 2. R+; 3. EA-; 4. V, VC, VG	*Homo sapiens*[b] (Mammalia, Primates)	Cali et al. (1998)

EA = exospore appendages; PE = protoplasmic extensions; PFC = polar filament coils; R = ridges; S = spores; Sp = sporonts; Spb = sporoblasts; T = tubular structures; V = individual vesicles; VC = vesicles in chains; VG = vesicles in globules; VT = vesiculartubular structures.

[a]Immunodeficient and immunocompetent patients, infected via bloodsucking dipterans.

[b]Single case in an immunodeficient patient, environmental source of infection is unknown.

species within the *Anncaliia* branch. The phylogenies based on this gene provided better resolution within *Nosema bombycis* clade as well (Kyei-Poku and Sokolova 2017).

The present finding of an *Anncaliia* species in an amphipod crustacean extends the natural host range of this genus. So far, *Anncaliia* spp. were recorded only as natural parasites of insects and etiological agents of opportunistic infections, that is, fatal myositis, in humans (Andreadis 2007; Cali et al. 2004; Coyle et al. 2004; Watts et al. 2014; Weiss 2014). It was shown by experiments that a broad range of hosts including gammarids easily acquired *A. algerae* infection after per oral or per cutaneous experimental challenge with spores (Becnel et al. 2005). This proves an extraordinary physiological plasticity of the representatives of this genus, limited neither by host body temperature nor by other physiological restraints. Given the possibility of human contacts with amphipod crustaceans abundant at some public beaches, microsporidia infections should be considered as a potential threat, especially when infected hosts are exposed to injured body parts, particularly of people belonging to "risky groups," such as immunodeficient individuals, elderly people, and young children.

Taxonomic considerations

Differential diagnosis

Gene sequences for SSU rRNA (KY288064), SSU-ITS-LSU rRNA (KY288065), HSP70 (KY288066), and RPB1 (KY288067) are the unique signatures that distinguish the microsporidium described herein from *A. algerae*, *A melighethi*, and the nomen nudum *V. algerae*. The gammarid microsporidium can also be differentiated from all known *Anncaliia* spp. by a crustacean host. Morphologically, the novel species differs from *A. algerae* by a longer polar filament, by the presence of exospore appendages in spores and sporoblasts, and by having protoplasmic extensions at proliferative stages. From *A. meligheti*, morphologically the most similar species, it differs by the structure of the appendages on the exospore. From *A. gambiae* and *A. vesicularum*, the described species can be differentiated by larger spores, a greater number of polar filament coils, and presence of exospore appendages; from *A. verivestis*, by the presence of exospore appendages and protoplasmic extensions at the proliferative stages. It differs from poorly morphologically characterized *A. connori* by slightly smaller size and fewer polar filament coils). Thus, the gammarid microsporidium from the Azov sea shore deserves the status of a new species of the genus *Anncaliia*. We describe it here under the name *Anncaliia azovica*.

TAXONOMIC SUMMARY

Phylum: Microsporidia Balbiani 1882
Family: Tubulinosematidae Franzen, Fischer, Schroeder, Scholmerich, Schneuwly 2005
Genus: *Anncaliia* Issi, Krylova, Nokolayeva 1993; emended by Franzen, Nassonova, Scholmerich, Issi 2006

Anncaliia azovica n. sp. Tokarev, Sokolova, Issi

Type host: *Niphargogammarus intermedius* Carausu 1943 (Crustacea, Amphipoda)
Type locality: Intertidal zone of Azov sea shore in the vicinity of village Achuevo, Slavyansk District of Krasnodar Territory, Russia
Cell and tissue tropism: Subcuticular fat body and myocytes
Pathology and types of secretion: Opaque colorations and swelling of infected tissues visible by unarmed eye. Secrete material seen on thin sections as circular profiles 40–80 nm, appear first on the plasma membrane of meronts. At the sporont and sporoblast stages this secretion form vesicular–tubular appendages composed of chains of round vesicles. Cytoplasm of infected cells is filled with the secretion formed by these chains, detached from the surfaces of sporonts and sporoblasts. Within the host cytoplasm, the chains can be seen whirled in globules up to 500 nm in diameter.
Interfacial envelopes at proliferative stages: All stages develop in direct contact with the host cell. Plasma membrane of meronts and sporonts is thickened. Sporont is enveloped by electron-dense amorphous material that forms ridges seen on transverse sections as wide indentations.
Life and nuclear cycle: is consistent with the genus diagnosis: diplokaryotic at all stages, monomorphic, monoxenic, disporoblastic.
Meronts: Round, oval, or of irregular shape; produce protoplasmic extensions.
Sporonts: Elongated cells with one diplokaryon and dense cytoplasm; divide by splitting the mother cell along the short axis; cellular and nuclear divisions are synchronized; may produce protoplasmic extensions.
Sporoblasts: Oval or elongated, with "waving" contours ("star-shaped" on cross-sections), undeveloped endospores and fully developed exospore with irregularly distributed appendages composed of vesicular–tubular secretion.
Spores: Spores are oval; live spores measured 5.1 ± 0.06 × 2.8 ± 0.03 μm, range 4.6–5.8 × 2.6–3.0 μm ($N = 20$); methanol-fixed spores measured 4.9 ± 0.08 × 2.8 ± 0.04 μm, range 4.5–5.7 × 2.4–3.2 μm ($N = 20$); on ultrathin sections—2.9–4.3 × 1.5–1.7 μm ($N = 6$). Endospore is about 100 nm thick (70–170) (in the apical region 0–20 nm). Exospore is 50 nm thick (44–46 nm), often ornamented with circular profiles 40–80 nm in diameter submerged into amorphous exospore matrix or attached to the surface. Spores are diplokaryotic. Anterior portion of polaroplast is built of tightly packed lamellae, posterior one—of broad saccules. Polar filament of 13–17 coils (median = 15), arranged in one row, with 0–4 (median = 3) posterior coils of lesser diameter.
Etymology: The species name alludes to the type locality, the Azov sea.
Gene sequences: GenBank accession numbers: KY288064 (SSU rRNA); KY288065 (SSU-ITS-LSU rRNA); KY288066 (HSP70); KY288067 (RPB1).

Zoobank registration number: urn:lsid:zoobank.org:act:1C645A27-F38C-4427-9944-464E85367D52

Type material: Type slides with methanol-fixed smears of infected gammarids containing spores and stages of the microsporidium are labeled "AZG-3." They are deposited in the microsporidia collection of the Institute of Plant Protection, St. Petersburg, Russia ("Dr. Issi's collection"). Embeddings, grids with thin sections, slides with thick sections, and images of thin sections labeled "*Anncaliia azovica* n. sp." are stored in the collection of YS.

ACKNOWLEDGMENTS

Authors are thankful to Yury Zuyev (State Research Institute of Lake and River Fisheries, St. Petersburg, Russia) for identification of the gammarid host and to Igor Senderskiy (All-Russian Institute for Plant Protection, St. Petersburg, Pushkin, Russia) for assistance with light microscopy. We acknowledge the use of Microscopy Center of the School of Veterinary Medicine, Louisiana State University, Baton Rouge, LA, USA. The research was supported by Russian Foundation for Basic Research, Project #17-04-00871.

LITERATURE CITED

Andreadis, T. G. 2007. Microsporidian parasites of mosquitoes. *J. Am. Mosq. Control Assoc.*, 23:3–29.

Becnel, J. J. & Andreadis, T. G. 1999. Microsporidia in insects. *In:* Wittner, M. & Weiss, L. M. (ed.), The Microsporidia and Microsporidiosis. American Society of Microbiology, Washington, DC. p. 447–501.

Becnel, J. J. & Andreadis, T. G. 2014. Microsporidia in insects. *In:* Weiss, L. M. & Becnel, J. J. (ed.), Microsporidia: Pathogens of Opportunity, 1st ed. Wiley Blackwell, Oxford. p. 521–570.

Becnel, J. J., White, S. E. & Shapiro, A. M. 2005. Review of microsporidia-mosquito relationships: from the simple to the complex. *Folia Parasitol.*, 52:41–50.

Brooks, W. M., Hazard, E. I. & Becnel, J. J. 1985. Two new species of *Noszema* (Microsporidia:Nosematidae) from the Mexican bean beetle *Epilachna varivestis* (Coleoptera: Coccinillidae). *J. Protozool.*, 32:525–535.

Cali, A., Takvorian, P. M., Lewin, S., Rendel, M., Sian, C. S., Wittner, M., Tanowitz, H. B., Keohane, E. & Weiss, L. M. 1998. *Brachiola vesicularum,* n. g., n. sp., a new microsporidium associated with AIDS and myositis. *J. Eukaryot. Microbiol.*, 45:240–251.

Cali, A., Weiss, L. M. & Takvorian, P. M. 2002. *Brachiola algerae* spore membrane systems, their activity during extrusion, and a new structural entity, the multilayered interlaced network, associated with the polar tube and the sporoplasm. *J. Eukaryot. Microbiol.*, 49:164–174.

Cali, A. N., Weiss, L. M. & Takvorian, P. M. 2004. An analysis of the microsporidian genus *Brachiola*, with comparisons of human and insect isolates of *Brachiola algerae*. *J. Eukaryot. Microbiol.*, 51:678–685.

Canning, E. U. & Sinden, R. E. 1973. Ultrastructural observations on the development of *Nosema algerae* Vavra and Undeen (Microsporidia: Nosematidae). *Protistologica*, 9:405–415.

Choudhary, M. M., Metcalfe, M. G., Arrambide, K., Bern, C., Visvesvara, G. S., Pieniazek, N. J., Bandea, R. D., DeLeon-Carnes, M., Adem, P., Choudhary, M. M., Zaki, S. R. & Saeed, M. U. 2011. *Tubulinosema* sp. microsporidian myositis in immunosuppressed patient. *Emerg. Infect. Dis.*, 17:1727–1730.

Coyle, C. M., Weiss, L. M., Rhodes, L. V., Cali, A., Takvorian, P. M., Brown, D. F., Visvesvara, G. S., Xiao, L., Naktin, J., Young, E., Gareca, M., Colasante, G. & Wittner, M. 2004. Fatal myositis due to the microsporidian *Brachiola algerae*, a mosquito pathogen. *N. Engl. J. Med.*, 351:42–47.

Franzen, C., Nassonova, E. S., Schölmerich, J. & Issi, I. V. 2006. Transfer of the members of the genus *Brachiola* (Microsporidia) to the genus *Anncaliia* based on ultrastructural and molecular data. *J. Eukaryot. Microbiol.*, 53:26–35.

Fries, I. 2010. *Nosema ceranae* in European honey bees (*Apis mellifera*). *J. Invertebr. Pathol.*, 103:S73–S79.

Hall, T. A. 1999. BioEdit: a user-friendly biological sequence alignment editor and analysis program for Windows 95/98/NT. *Nucleic Acids Symp. Ser.*, 41:95–98.

Issi, I. V., Krylova, S. V. & Nicolaeva, V. M. 1993. The ultrastructure of the microsporidium *Nosema meligheti* and establishment of the new genus *Anncaliia*. *Parazitologiia*, 27:127–133 (in Russian with English summary).

Kent, M. L., Shaw, R. W. & Sanders, J. L. 2014. Microsporidia in fish. *In:* Weiss, L. & Becnel, J. J. (ed.), Microsporidia: Pathogens of Opportunity, 1st ed. Wiley Blackwell, Oxford. p. 493–520.

Kimura, M. 1980. A simple method for estimating evolutionary rates of base substitutions through comparative studies of nucleotide sequences. *J. Mol. Evol.*, 16:111–120.

Koudela, B., Visvesvara, G. S., Moura, H. & Vávra, J. 2001. The human isolate of *Brachiola algerae* (Phylum Microspora): development in SCID mice and description of its fine structure features. *Parasitology*, 123:153–162.

Kumar, S., Stecher, G. & Tamura, K. 2015. MEGA7: molecular evolutionary genetics analysis version 7.0. *Mol. Biol. Evol.*, 33:1870–1874.

Kyei-Poku, G. & Sokolova, Y. Y. 2017. The microsporidium *Nosema disstriae* (Thomson 1959): fine structure and phylogenetic position within the *N. bombycis* clade. *J. Invertebr. Pathol.*, 143:90–103.

Margileth, A. M., Strano, A. J., Chandra, R., Neafie, R., Blum, M. & McCulli, R. M. 1973. Disseminated nosematosis in an immunologically compromised patient. *Arch. Pathol.*, 95:145–150.

Meissner, E. G., Bennett, J. E., Qvarnstrom, Y., da Silva, A., Chu, E. Y., Tsokos, M. & Gea-Banacloche, J. 2012. Disseminated microsporidiosis in an immunosuppressed patient. *Emerg. Infect. Dis.*, 18:1155–1158.

Monaghan, S. R., Rumney, R. L., Vo, N. T. K., Bols, N. C. & Lee, L. E. J. 2011. In vitro growth of microsporidia *Anncaliia algerae* in cell lines from warm water fish. *In Vitro Cell. Dev. Biol. Anim.*, 47:104–113.

Mordukhai-Boltovskoi, F. D., Greze, I. I. & Vasilenko, S. V. 1969. Order Amphipoda Latreille 1816–1817. *In:* Vodjanickij, V. A. (ed.), Guide to the Fauna of the Black and Azov Sea, Vol. 2. Free-living invertebrates: crustaceans. Naukova Dumka, Kiev. p. 440–524 (in Russian).

Pariyakanok, L., Satitpitakul, V., Putaporntip, C. & Jongwutiwes, S. 2015. Femtosecond laser-assisted anterior lamellar keratoplasty in stromal keratitis caused by an *Endoreticulatus*-like microsporidia. *Cornea*, 34:588–591.

Ronquist, F., Teslenko, M., Van Der Mark, P., Ayres, D. L., Darling, A., Höhna, S., Larget, B., Liu, L., Suchard, M. A. & Huelsenbeck, J. P. 2012. Mrbayes 3.2: Efficient Bayesian phylogenetic inference and model choice across a large model space. *Syst. Biol.*, 61:539–542.

Shadduck, J. A., Kelsoe, G. & Helmke, R. J. 1979. A microsporidian contaminant of a non-human primate cell culture: ultrastructural comparison with *Nosema connori*. *J. Parasitol.*, 65:185–188.

Sokolova, Y. Y. 2015. Perspectives of microsporidia as human pathogens: clues from invertebrate research (minireview). *Protistology*, 9:117–126.

Sokolova, Y. Y., Dolgikh, V. V., Morzhina, E. V., Nassonova, E. S., Issi, I. V., Terry, R. S., Ironside, J. E., Smith, J. E. & Vossbrinck, C. R. 2003. Establishment of the new genus *Paranosema* based on the ultrastructure and molecular phylogeny of the type species *Paranosema grylli* Gen. Nov., Comb. Nov. (Sokolova, Selezniov, Dolgikh, Issi 1994), from the cricket *Gryllus bimaculatus* Deg. *J. Invertebr. Pathol.*, 84:159–172.

Sokolova, Y. Y. & Fuxa, J. R. 2008. Biology and life-cycle of the microsporidium *Kneallhazia solenopsae* Knell Allan Hazard 1977 gen. n., comb. n., from the fire ant *Solenopsis invicta*. *Parasitology*, 135:903–929.

Sokolova, Y. Y., Lange, C. E., Mariottini, Y. & Fuxa, J. R. 2009. Morphology and taxonomy of the microsporidium Liebermannia covasacrae n. sp. from the grasshopper *Covasacris pallidinota* (Orthoptera, Acrididae). *J. Invertebr. Pathol.*, 101:34–42.

Sprague, V. 1974. *Nosema connori* n.sp., a microsporidian parasite of man. *Trans. Am. Microsc. Soc.*, 93:400–403.

Stentiford, G. D., Feist, S. W., Stone, D. M., Bateman, K. S. & Dunn, A. M. 2013. Microsporidia: diverse, dynamic, and emergent pathogens in aquatic systems. *Trends Parasitol.*, 29:567–578.

Suankratay, C., Thiansukhon, E., Nilaratanakul, V., Putaporntip, C. & Jongwutiwes, S. 2012. Disseminated infection caused by novel species of Microsporidium, Thailand. *Emerg. Infect. Dis.*, 18:302–304.

Takvorian, P. M., Buttle, K. F., Mankus, D., Mannella, C. A., Weiss, L. M. & Cali, A. 2013. The multilayered interlaced network (MIN) in the sporoplasm of the microsporidium *Anncaliia algerae* is derived from Golgi. *J. Eukaryot. Microbiol.*, 60:166–178.

Takvorian, P. M., Weiss, L. M. & Cali, A. 2005. The early events of *Brachiola algerae* (Microsporidia) infection: spore germination, sporoplasm structure, and development within host cells. *Folia Parasitol.*, 52:118–129.

Tamura, K., Peterson, D., Peterson, N., Stecher, G., Nei, M. & Kumar, S. 2011. MEGA5: Molecular evolutionary genetics analysis using maximum likelihood, evolutionary distance, and maximum parsimony methods. *Mol. Biol. Evol.*, 28:2731–2739.

Tokarev, Y. S., Voronin, V. N., Seliverstova, E. V., Dolgikh, V. V., Pavlova, O. A., Ignatieva, A. N. & Issi, I. V. 2010. Ultrastructure and molecular phylogeny of *Anisofilariata chironomi* sp.n. g.n. (Microsporidia: Terresporidia), a microsporidian parasite of *Chironomus plumosus* L. (Diptera: Chironomidae). *Parasitol. Res.*, 107:39–46.

Trammer, T., Chioralia, G., Maier, W. A. & Seitz, H. M. 1999. In vitro replication of *Nosema algerae* (Microsporidia), a parasite of anopheline mosquitoes, in human cells above 36°C. *J. Eukaryot. Microbiol.*, 46:464–468.

Vávra, J., Horák, A., Modrý, D., Lukeš, J. & Koudela, B. 2006. *Trachipleistophora extenrec* n. sp. a new microsporidian (Fungi: Microsporidia) infecting mammals. *J. Eukaryot. Microbiol.*, 53:464–476.

Vávra, J., Kamler, M., Modrý, D. & Koudela, B. 2011. Opportunistic nature of the mammalian microsporidia: experimental transmission of *Trachipleistophora extenrec* (Fungi: Microsporidia) between mammalian and insect hosts. *Parasitol. Res.*, 108:1565–1573.

Vávra, J., Yachnis, A. T., Shadduck, J. A. & Orenstein, J. M. 1998. Microsporidia of the genus *Trachipleistophora* – causative agents of human microsporidiosis: description of *Trachipleistophora anthropophthera* n. sp. (Protozoa: Microsporidia). *J. Eukaryot. Microbiol.*, 45:273–283.

Visvesvara, G. S., Moura, H., Leitch, G. J. & Schwartz, D. A. 1999. Culture and propogation of microsporidia. *In:* Wittner, M. & Weiss, L. (ed.), The Microsporidia and Microsporidiosis. ASM press, Washington, DC. p. 363–392.

Vossbrinck, C. R. & Debrunner-Vossbrinck, B. A. 2005. Molecular phylogeny of the Microsporidia: ecological, ultrastructural and taxonomic considerations. *Folia Parasitol.*, 52:131–142.

Watts, M. R., Chan, R. C. F., Cheong, E. Y. L., Brammah, S., Clezy, K. R., Tong, C., Marriott, D., Webb, C. E., Chacko, B., Tobia, V., Outhred, A. C., Field, A. S., Prowse, M. V., Bertouch, J. V., Stark, D. & Reddel, S. W. 2014. *Anncaliia algerae* microsporidial myositis. *Emerg. Infect. Dis.*, 20:185–191.

Weidner, E., Canning, E. U., Rutledge, C. R. & Meek, C. L. 1999. Mosquito (Diptera: Culicidae) host compatibility and vector competency for the human myositic parasite *Trachipleistophora hominis* (Phylum Microspora). *J. Med. Entomol.*, 36:522–525.

Weiser, J. & Žižka, Z. 2004. *Brachiola gambiae* sp. n., the microsporidian parasite of *Anopheles gambiae* and *A. melas* in Liberia. *Acta Protozool.*, 43:73–80.

Weiss, L. M. 2014. Clinical syndromes associated with microsporidiosis. *In:* Weiss, L. & Becnel, J. J. (ed.), Microsporidia: Pathogens of Opportunity, 1st ed. Wiley Blackwell, Oxford. p. 371–401.

Weiss, L. M. & Vossbrinck, C. R. 1999. Molecular biology, molecular phylogeny, and molecular diagnostic approaches to the Microsporidia. *In:* Wittner, M. & Weiss, L. (ed.), The Microsporidia and Microsporidiosis. ASM Press, Washington, DC. p. 129–171.